ChemComm

Accepted Manuscript

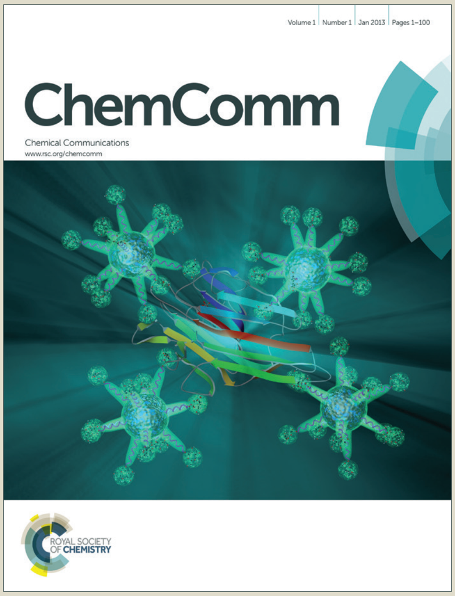

ROYAL SOCIETY OF CHEMISTRY

www.rsc.org/chemcomm

Journal Name
RSCPublishing

COMMUNICATION

Cite this: DOI: 10.1039/x0xx00000x

Metal ion promoted tautomerization and C-N bond cleavage: conversion of catechol to a *p*-benzoquinone derivative[†]

Received 00th January 2012,
Accepted 00th January 2012

DOI: 10.1039/x0xx00000x

www.rsc.org/

Pinaki Saha,[a] Amit Saha Roy,[a] Thomas Weyhermüller[b] and Prasanta Ghosh*[a]

Metal ion promoted *p*-iminoquinone to *o*-diiminoquinone tautomerization and a C-N bond cleavage of 2,5-bis(*p*-tolylamino)-4-*p*-tolyliminobenzoquinone leading to the conversion of catechol to a *p*-benzoquinone derivative are reported.

Catechols and *p*-benzoquinones are redox active agents which participate in several biological electron transfer reactions.[1,2] Although the transformations of catechols to *o*-benzoquinones and *p*-hydroquinones to *p*-benzoquinones and *vice versa* are common in chemistry, the interconversion of catechol to *p*-benzoquinone is not achieved so far. In this communication, we report the conversion of catechol to a *p*-quinone derivative by two-step reactions which involve the transformation of catechol to 2,5-bis(*p*-tolylamino)-4-*p*-tolyliminobenzoquinone ($Q_{p\text{-NO}}$) followed by a metal promoted tautomerization and a C-N bond cleavage leading to the formation of a *p*-benzoquinone derivative. The metal promoted conversion/interconversion of redox non-innocent quinone ligands is relevant to predict the structures of the quinoproteins[3] and the area is a subject of topical interest to model tautomeric molecular switches[4] and new coordination complexes.[5] Metal promoted tautomerization was reported first by Kaim *et al*[6] in an azophenine ligand having ground electronic state similar to $Q_{p\text{-NO}}$. Recently, the coordination chemistry of azophenine,[7] 2,5-diamino-1,4-benzoquinonediimine,[8] 1,2,4,5-tetra(alkylamine)benzene[9] and zwitterionic *N*-substituted benzoquinone monoimine[10] as bridging ligands in different aspects was reported. The coordination chemistry of $Q_{p\text{-NO}}$[11] is not explored so far.

In this investigation, palladium(II) ion promoted tautomerization of $Q_{p\text{-NO}}$ to 3-hydroxy-4-(*p*-tolylamino)-*o*-bis(*p*-tolylimino benzoquinone) ($Q_{o\text{-NN}}$) affording [$Pd^{II}(Q_{o\text{-NN}})Cl_2$] (**1**) in good yields was authenticated. The similar reaction of $Q_{p\text{-NO}}$ with $RhCl_3$ in presence of PPh_3 as co-ligands in moist MeCN/EtOH progresses further surprisingly with a C-N bond cleavage affording [$Rh^{III}(PPh_3)$(*p*-toluidine)(MeCN)Cl_3] (**2**) and 2,5-bis(*p*-tolylamino)-*p*-benzoquinone ($Q_{p\text{-OO}}$)[12] as products as shown in Scheme 1. Details of all the synthetic reactions are outlined in the experimental section (ESI[†]). The probable paths of formation of $Q_{p\text{-NO}}$ from catechol are depicted in Scheme 2.

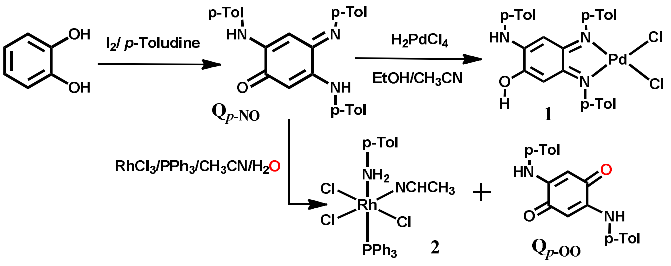

Scheme 1

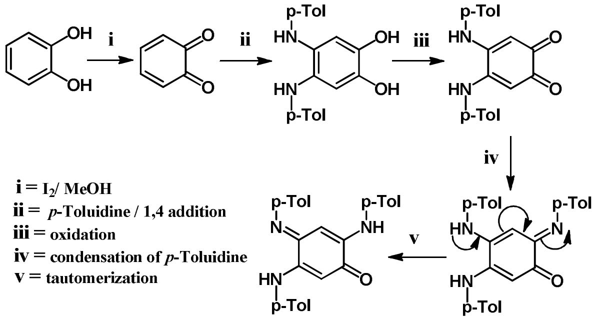

Scheme 2

The tautomerization and the cleavage reaction of $Q_{p\text{-NO}}$ as illustrated in Scheme 1 were established by the isolations of the related products which were characterized by the analytical data, IR, mass, ^1H and ^{13}C NMR, UV-vis absorption spectra including the single crystal X-ray structure determinations of $Q_{p\text{-NO}}$, **1** and **2**. Energies of the tautomers of $Q_{p\text{-NO}}$ and $Q_{o\text{-NN}}$ are analyzed by the density functional theory (DFT) calculations at

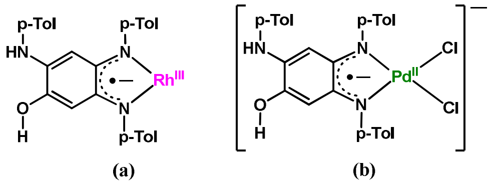

Chart 1

the B3LYP level of the theory (*vide infra*).

The coordination of palladium(II) ion to $Q_{p\text{-NO}}$ promotes a proton transfer generating $Q_{o\text{-NN}}$ complex of palladium(II) ion. On the contrary, the reaction of $Q_{p\text{-NO}}$ with $RhCl_3$ and PPh_3 as co-ligands in moist MeCN/EtOH mixture promotes the tautomerization and a hydrolytic cleavage of the coordinated =N-*p*-tol group trans to keto group producing *p*-benzoquinone ($Q_{p\text{-OO}}$) and *p*-toluidine which coordinates to rhodium(III) ion affording orange **2**. The reaction progresses with a diiminobenzosemiquinone anion radical[13] intermediate of rhodium (III) ion (Chart 1(a)) detected by the EPR spectrum of the frozen reaction mixture at 150 K with the *g* parameter at 1.996 as shown in Fig. 1(a). The probable paths of the cleavage reaction are depicted in Scheme 3. It is noteworthy that under this experimental condition (1:1 acetonitrile and ethanol and without rhodium precursor), $Q_{p\text{-NO}}$ does not undergo any hydrolysis reaction. In dry solvents and in absence of moisture, **2** was not obtained. It is observed that the reaction of $RhCl_3$ with PPh_3 and *p*-toluidine affords **2**, similarly the reaction of $H_2[PdCl_4]$ with *p*-toluidine produces *trans*-$[PdCl_2(p\text{-toluidine})_2]$.[14] However, boiling of **1** in MeCN/EtOH mixture does not undergo any cleavage reaction inferring that the hydrolytic cleavage reaction is rhodium ion selective.

The $Q_{p\text{-OO}}$ exhibits the mass peak (*m/z*) at 317.96 and 316.95 (Fig. S1, ESI†); the calculated mass of $Q_{p\text{-OO}}$ is 318.14. The absorption bands due to stretching vibrations of C=O and N-H of $Q_{p\text{-OO}}$ appear at 1726, 1634 cm^{-1} and 3252 cm^{-1}. ^1H and ^{13}C NMR spectral data which are summarized in the experimental section compare well with those reported by Bergman *et. al.*[12] The $\nu_{N\text{-}H}$ of $Q_{p\text{-NO}}$ appears at 3313 and 3282 cm^{-1}, whereas in $Q_{o\text{-NN}}$ of **1**, it shifts to 3244 cm^{-1}. The ν_{OH} is observed at 3434 cm^{-1}. **2** exhibits absorption band at 3255 and 3131 cm^{-1} characteristically due to symmetric and anti-symmetric stretching vibrations of the coordinated $-NH_2$ group. The UV-vis absorption spectra of $Q_{p\text{-NO}}$, **1** and **2** in CH_2Cl_2 are shown in Fig. 2. $Q_{p\text{-NO}}$ absorbs with the λ_{max} at 544 and 392 nm, while **1** displays band with the maxima at 671, 617 and 452 nm as listed in Fig. 2. The lower energy absorption bands are absent in **2** which absorbs strongly at 303 nm (Fig. 2).

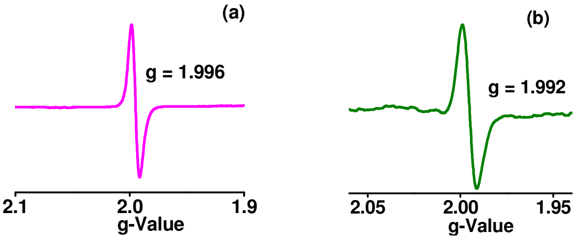

Fig. 1 X-band EPR spectra of (a) the frozen reaction mixture following the formation of **2** in MeCN at 150 K (frequency = 9.44344 GHz) and (b) $[\mathbf{1}]^-$ in DMF solvent at 298 K (frequency = 9.446408 GHz).

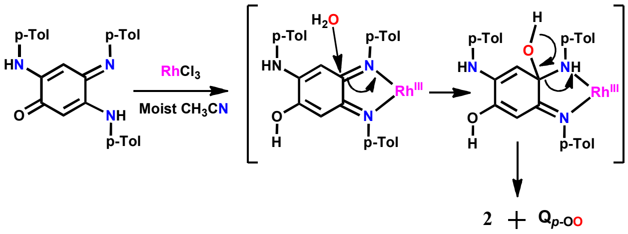

Scheme 3

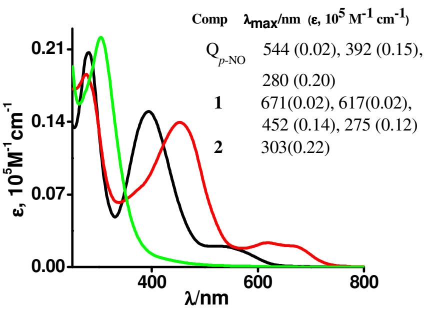

Comp	λ_{max}/nm (ε, $10^5\ M^{-1}\ cm^{-1}$)
$Q_{p\text{-NO}}$	544 (0.02), 392 (0.15), 280 (0.20)
1	671(0.02), 617(0.02), 452 (0.14), 275 (0.12)
2	303(0.22)

Fig. 2 UV-vis absorption spectra of $Q_{p\text{-NO}}$ (black), **1** (red) and **2** (green) in CH_2Cl_2 at 298 K.

The molecular geometries and the bond parameters of $Q_{p\text{-NO}}$, **1** and **2** were confirmed by single crystal X-ray structure determinations (crystallographic data are listed in Table S1, ESI†). $Q_{p\text{-NO}}$.MeCN crystallizes in *P*-1 space group. The molecular geometry in crystals and the atom labelling scheme are

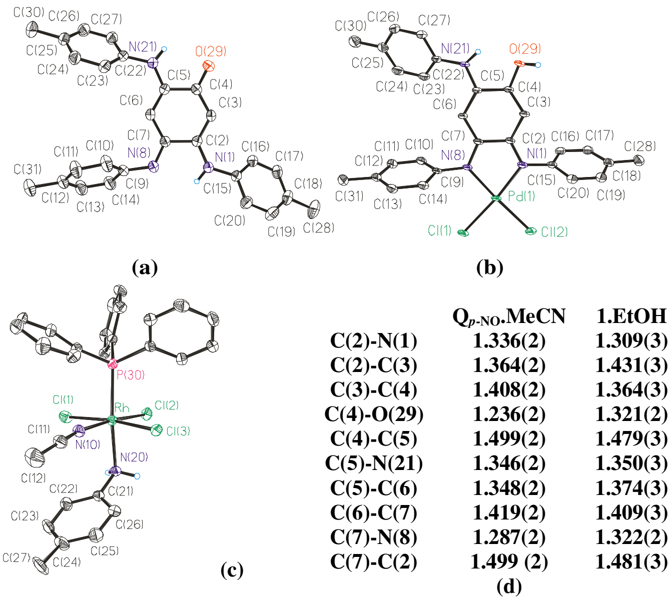

	$Q_{p\text{-NO}}$.MeCN	1.EtOH
C(2)-N(1)	1.336(2)	1.309(3)
C(2)-C(3)	1.364(2)	1.431(3)
C(3)-C(4)	1.408(2)	1.364(3)
C(4)-O(29)	1.236(2)	1.321(2)
C(4)-C(5)	1.499(2)	1.479(3)
C(5)-N(21)	1.346(2)	1.350(3)
C(5)-C(6)	1.348(2)	1.374(3)
C(6)-C(7)	1.419(2)	1.409(3)
C(7)-N(8)	1.287(2)	1.322(2)
C(7)-C(2)	1.499 (2)	1.481(3)

(d)

Fig. 3 Molecular geometries of (a) $Q_{p\text{-NO}}$.MeCN (b) **1**.EtOH (Pd(1)-N(1), 2.010(2); Pd(1)-N(8), 2.017(2); Pd(1)-Cl(1), 2.278(1); Pd(1)-Cl(2), 2.286(1)) and (c) **2** (Rh-N(20), 2.162(4); Rh-N(10), 2.017(4); Rh-P(30), 2.307(2); Rh-Cl(1), 2.397(2); Rh-Cl(2), 2.314(2); Rh-Cl(3), 2.371(2)) in crystals (H atoms and solvents are omitted for clarity) (d) comparison of significant bond lengths of $Q_{p\text{-NO}}$.MeCN and **1**.EtOH.

depicted in Fig. 3(a). Significant bond parameters are summarized in the panel (d) of Fig. 3. The bond length trend with the quinoidal distortion of the central phenyl ring corroborates well with the *p*-iminobenzoquinone state of the ligand. C(7)-N(8) and C(4)-O(29) lengths are 1.287(2) and 1.236(2) Å. The C(2)-C(3) and C(5)-C(6) bond lengths are relatively shorter than those observed in an aromatic ring. However, the C(4)-C(5) and C(2)-C(7) lengths are longer than average aromatic C-C lengths. In comparison to those expected in an aromatic amine compound, C(2)-N(1) and C(5)-N(21) bonds in $Q_{p\text{-NO}}$.MeCN are shorter. The length trend predicts a two halves five-centered $6\pi e$ delocalization: one half is constituted of N(1)-C(2)-C(3)-C(4)-O(29) and another is constituted of N(8)-C(7)-C(6)-C(5)-N(21) atoms, which are relevant to $Q_{p\text{-NO}}$ state.

1.EtOH crystallizes in P-1 space group. The molecular geometry and the atom labelling scheme are shown in Fig. 3(b). The significant bond parameters are listed in panel (d) and under the caption of Fig. 3. PdN_2Cl_2 sites including the central phenyl ring are planar. Significant changes of the C(4)-O(29) and C(2)-N(1) bond lengths in going from $Q_{p\text{-NO}}$.MeCN to **1**.EtOH are recorded. In **1**.EtOH, C(4)-O(29) lengthens to 1.321(2) from 1.237(2) Å, while the C(2)-N(1) length shortens to 1.309(3) from 1.335(2) Å that is observed in $Q_{p\text{-NO}}$.MeCN. The C-N and C-O bond length features in **1**.EtOH do not correlate with the $Q_{p\text{-NO}}$ tautomer. C(4)-O(29) length is much longer than a C=O length, while the C(5)-N(21) length, 1.350(3) Å, does not change notably. The C(7)-N(8) bond length is 1.322(2) Å. Further, the shortening of C(3)-C(4) length is consistent with the existence of $Q_{o\text{-NN}}$ state of the ligand in **1**.EtOH. Metrical parameter analysis affirmed the tautomerization of the $Q_{p\text{-NO}}$ to $Q_{o\text{-NN}}$ state in **1**.EtOH. In **1**.EtOH, the two halves five-centered $6\pi e$ delocalization units which correlate to the $Q_{o\text{-NN}}$ state are N(1)-C(2)-C(3)-C(4)-O(29) and N(8)-C(7)-C(6)-C(5)-N(21) (*vide infra*).

2 crystallizes in $P2_1/c$ space group. The molecular geometry and the atom labelling scheme of **2** are illustrated in Fig. 3(c) and the bond parameters of the coordination sphere are listed under the caption of Fig. 3. The MeCN molecule coordinates almost linearly with a Rh-N-C angle of 170.1° while the *p*-toluidine molecules coordinates angularly with a Rh-N-C angle of 119.2° (Table S4, ESI†).

The redox activities of $Q_{p\text{-NO}}$ and **1** were investigated by cyclic voltammometry. The redox potential data referenced to the ferrocenium/ferrocene, Fc^+/Fc, couple are summarized in Table 1 and the voltammograms are shown in Fig. S2. The anodic waves of both the molecules are irreversible, while the cathodic wave of **1** at -1.33 V is quasireversible. EPR spectrum of [**1**]$^-$ at 298 K (Fig. 1(b)) corresponding to the g value at 1.992 authenticated that the cathodic peak is because of the $Q_{o\text{-NN}}^{\bullet-}/Q_{o\text{-NN}}$ couple. $Q_{o\text{-NN}}^{\bullet-}$ is a diiminobenzosemiquinone anion radical[13] as shown in Chart 1(b) and [**1**]$^-$ is defined as $[Pd(Q_{o\text{-NN}}^{\bullet-})Cl_2]^-$.

Table 1 Redox potential data of $Q_{p\text{-NO}}$ and **1** at 298 K

Comp.	Solvent	$E_p{}^a$,V (+1/0)	$E_{1/2}$,V (0/-1)
$Q_{p\text{-NO}}$	CH_3CN	0.50	-1.43^b
	DMSO	0.61	-1.37^b
1	DMF	-0.30	-1.33 (220 mV)^c

^{a}anodic peak, ^{b}cathodic peak, ^{c}peak-to-peak separation

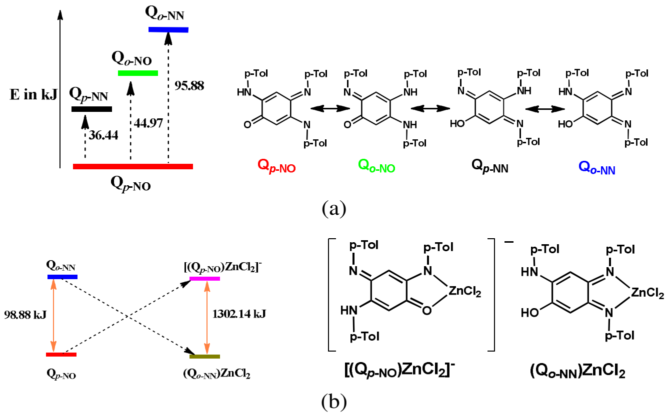

Chart 2

Ground state energies of the four tautomers, $Q_{p\text{-NO}}$, $Q_{o\text{-NN}}$, $Q_{p\text{-NN}}$, $Q_{o\text{-NO}}$ as illustrated in Chart 2(a) are calculated at the B3LYP/DFT level (Tables S5-S12, ESI†). The calculations reveal the minimum ground state energy of the $Q_{p\text{-NO}}$ tautomer while upon coordination to a zinc(II) ion having crystal field stabilization energy zero, $Q_{o\text{-NN}}$ tautomer has the least energy as shown in Chart 2(b). The observations correlate well with the isolation of $Q_{p\text{-NO}}$ as the only quinone derivative that turns to $Q_{o\text{-NN}}$ tautomer in **1** (Chart 2(a)). Molecular orbital analyses have detected the two halves five-centered delocalization units in $Q_{p\text{-NO}}$ and **1**, which are illustrated in Fig. 4. The features are consistent with the bond parameters obtained from the single crystal X-ray determinations of $Q_{p\text{-NO}}$.MeCN and **1**.EtOH as listed in Tables S2-S3 (ESI†). TD DFT calculations elucidated that the lower energy absorption band of **1** which is absent in $Q_{p\text{-NO}}$, is because of the palladium (II) ion to $Q_{o\text{-NN}}$ charge transfer (Tables S13-S14 and Fig. S3-S4, ESI†).

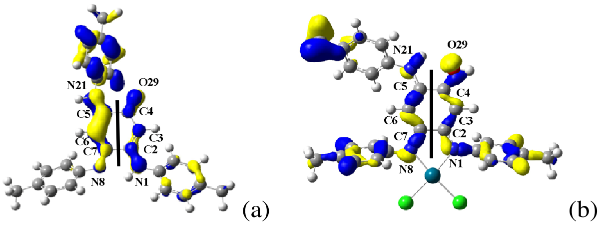

Fig. 4 Two halves five-centered delocalization units in (a) $Q_{p\text{-NO}}$ and (b) **1**

Conclusion

In conclusion, a path of conversion of catechol to *p*-quinone derivatives is authenticated.

Financial support received from DST (SR/S1/IC/0026/2012) and CSIR 01(2699/12/EMR-II) New Delhi, India is gratefully acknowledged. PS is (CSIR, 01(2699/12/EMR-II)) thankful to CSIR for fellowships (SRF).

Notes and references

[a]Department of Chemistry, R. K. Mission Residential College, Narendrapur, Kolkata-103, India. E-mail: ghosh@pghosh.in; Fax: +913324773597; Tel: +913324287347. [b]Max-Planck-Institut für Chemische Energiekonversion, Stiftstrasse 34-36 / D-45470 Mülheim an der Ruhr, Germany.

[†]Electronic Supplementary Information (ESI) available: [Materials, syntheses, physical measurements, ESI mass spectrum of $Q_{p\text{-OO}}$ (Fig. S1), X-ray crystallographic data of $Q_{p\text{-NO}}$.MeCN, **1**.EtOH and **2**: CCDC numbers 979387-979389, Table S1, selected experimental and calculated bond parameters (Tables S2-S4), cyclic voltammograms (Fig. S2), DFT calculations: gas phase optimized coordinates of $Q_{p\text{-NO}}$, $Q_{p\text{-NN}}$, $Q_{o\text{-NO}}$, $Q_{o\text{-NN}}$, **1**, $\mathbf{2}^{\mathbf{Me}}$, $[(Q_{o\text{-NN}})ZnCl_2]$ and $[(Q_{o\text{-NO}})ZnCl_2]^-$ (Tables S5-S12), electronic transitions of $Q_{p\text{-NO}}$ and **1** based on TD DFT calculations (Tables S13-S14 and Fig. S3-S4). See DOI: 10.1039/c000000x/

1 (a) W. Kaim and B. Schwederski, *Coord. Chem. Rev.*, 2010, **254**, 1580; (b) C. G. Pierpont, *Coord. Chem. Rev.*, 2001, **216-217**, 99; (c) J. Q. Chambers, in *The Chemistry of Quinonoid Compounds*, ed. S. Patai and Z. Rappaport, Wiley, New York, 1988, Vol. II, p 719; (d) C. G. Pierpont and R. M. Buchanan, *Coord. Chem. Rev.* 1981, **38**, 45-87.

2 J. R. Bolton, N. Mataga and G. McLendon, eds., in *Electron Transfer in Inorganic, Organic and Biological Systems,* American Chemical Society, Washington DC, 1991, Volume 228.

3 (a) C. Anthony, *Biochem. J.*, 1996, **320**, 697-711; (b) P. R. Rich, *Faraday Discuss. Chem. Soc.*, 1982, **74**, 349-364.

4 G. J. Simpson, S. W. L. Hogan, M. Caffio, C. J. Adams, H. Früchtl, T. van Mourik and R. Schaub, *Nano Lett.*, 2014, **14**, 634-639.

5 S. Wirth, A. U. Wallek, A. Zernickel, F. Feil, M. S. -Sikorska, K. L. -Mieczkowska, C. Bräuchle, I. -P. Lorenz and M. Czyz, *J. Inorg. Biochem.*, 2010, **104**, 774-789.

6 (a) S. Frantz, J. Rall, I. Hartenbach, T. Schleid, S. Zalis and W. Kaim, *Chem. Eur. J.*, 2004, **10**, 149; (b) J. Rall, A. F. Stange, K. Hübler and W. Kaim, *Angew. Chem. Int. Ed.*, 1998, **37**, 2681-2682.

7 I. -R. Jeon, J. G. Park, D. J. Xiao and T. D. Harris, *J. Am. Chem. Soc.,* 2013, **135**, 16845.

8 (a) Y. -B. Huang, G. -R. Tang, G. -Y. Jin and G. –X. Jin, *Organometallics*, 2008, **27**, 259-269; (b) J. -P. Taquet, O. Siri, R. Welter and P. Braunstein, *Inorg. Chem.*, 2006, **45**, 4668-4676.

9 S. Krupski, J. V. Dickschat, A. Hepp, T. Pape and F. E. Hahn, *Organometallics*, 2012, **31**, 2078-2084.

10 (a) A. Ghisolfi, A. Waldvogel, L. Routaboul and P. Braunstein, *Inorg. Chem.*, 2014, **53**, 5515-5526; (b) P. Braunstein, D. Bubrin and B. Sarkar, *Inorg. Chem.*, 2009, **48**, 2534; (c) P. Braunstein, O. Siri, J. -P. Taquet, M. -M. Rohmer, M. Benard and R. Welter, *J. Am. Chem. Soc.*, 2003, **125**, 12246-12256.

11 (a) S. G. Pyne and R. J. W. Truscott, *Tetrahedron*, 1990, **46**, 661; (b) K. Balenovic, R. Lazic, V. Polak and P. Stern, *Bull. Sci., Cons. Acad. Sci. Arts RSF Yougoslavia Sect. A*, 1972, **17**, 147.

12 J. Bergman, L. N. Yudina, J. Tholander and G. Lidgren, *Tetrahedron*, 2002, **58**, 1443.

13 (a) K. Chłopek, E. Bill, T. Weyhermüller and K. Wieghardt, *Inorg. Chem.*, 2005, **44**, 7087; (b) P. Ghosh, A. Begum, D. Herebian, E. Bothe, P. Hildenbrand, T. Weyhermuller and K. Wieghardt, *Angew. Chem., Int. Ed.,* 2003, **42**, 563; (c) A. L. Balch and R. H. Holm, *J. Am. Chem. Soc.,* 1966, **88**, 5201.

14 N. Kumari, V. K. Jadav, S. Zalis and L. Mishra, *Ind. J Chem.,* 2012, **51A**, 554-563.